SPECIAL CONCENTRICALLY BRACED FRAME FUNCTIONAL RECOVERY PREQUALIFICATION

Final Report Submitted to the PUC (1/5/2026) for Consideration in the 2026 NEHRP Provisions

FUNCTIONAL RECOVERY PREQUALIFICATION REPORT FOR SPECIAL CONTRENTRICALLY BRACED FRAMES

Final Report Submitted to the PUC for Consideration in the 2026 NEHRP Provisions

Prepared By:

Resilient Design Coalition

Financially Supported by:

American Institute of Steel Construction and the Charles Pankow Foundation

TECHNICAL WORK AND AUTHORSHIP BY:

Ed Almeter, MS
Kristen Blowes, PhD, PE
Jared DeBock, PhD, PE
Curt Haselton, PhD, PE
Carlos Molina Hutt, PhD, PE
Huy Pham, PhD
David Welch, PhD
Reid Zimmerman, SE

January 5, 2026

QUANTIFICATION OF FUNCTIONAL RECOVERY SEISMIC PERFORMANCE FACTORS FOR CONCENTRICALLY BRACED FRAMES

Submitted: 1/5/2026

EXECUTIVE SUMMARY

A quantification of the functional recovery seismic performance factors for the Special Concentrically Braced Frame (SCBF) lateral force-resisting system is performed in accordance with the proposed Section A.8.3.6 procedures in Appendix A of the 2026 National Earthquake Hazards Reduction Program (NEHRP) Provisions. The assessments documented herein cover the design of buildings with SCBF lateral force-resisting systems in accordance with Chapter 12 of ASCE 7-22. Only SCBF structures up to 10 stories tall were studied. Therefore, the recommended functional recovery performance factors apply only to SCBF structures with 10 or fewer stories. Additionally, all SBFS systems assessed comply with new seismic compactness limits (b/t) currently under ballot for adoptions into the 2027 AISC Seismic Provisions (AISC, 2025). Design coefficients and factors for life-safety design are based on line B.2 of Table 12.2-1 in ASCE 7-22, "Steel special concentrically braced frames." The response modification coefficient, R, is 6, the overstrength factor, Ω, is 2, and the deflection amplification factor, C_d, is 5. All designs investigated herein satisfy the life-safety design provisions of ASCE 7-22.

Appendix A of the 2026 NEHRP Provisions provides additional design requirements to satisfy functional recovery performance objectives at the Functional Recovery Earthquake (FRE_R) level shaking. The functional recovery seismic performance factors include the functional recovery response modification coefficient, R_{fr}, functional recovery allowable story drift limit, Δ_{afr}, and the functional recovery structure ductility reduction factor, $R_{\mu fr}$. Drift checks are performed with the functional recovery deflection amplification factor, C_{dfr} equal to R_{fr} for functional recovery design.

R_{fr} and Δ_{afr} were determined by developing an archetype space of different building heights, designed with various functional recovery response modification coefficients and allowable drift limits, and then selecting the combination that results in less than a 10% mean probability of Safety-Critical Structural Damage, or P[SCSD], in each performance group, and less than 20% P[SCSD] for any individual archetype, for Functional Recovery Category (FRC) A, B and C. The 10% and 20% thresholds are modified to 15% and 25%, respectively, for FRC D. All analyses are conducted at the Functional Recovery Earthquake (FRE_R) level shaking corresponding to a Seismic Design Category $D_{max,FRE}$ condition with two-point spectral ordinates S_{dsfr} and S_{d1fr} of 1.25g and 0.75g, respectively. The required values of R_{fr} and Δ_{afr} based on analysis are compared to the judgment-based limits according to Appendix A of NEHRP 2026, and the more stringent values are selected. The judgment-based limits of R_{fr} are R/1.5 and R/1.25 for FRC A/B/C and FRC D, respectively. The judgment-based limits of Δ_{afr} are 1.25% and 1.75%

for FRC A/B/C and FRC D, respectively. System specific $R_{\mu fr}$ factors are determined by comparing peak floor acceleration demands from the analysis with the seismic floor accelerations from Section A.10.6 in accordance with the procedures in Section A.8.3.6 in Appendix A of the 2026 NEHRP Provisions.

The proposed R_{fr}, Δ_{afr} and $R_{\mu fr}$ for the SCBF lateral force-resisting system from the qualification assessment are presented in Table 1. Results from the assessment showed that the functional recovery performance factors for SCBFs were governed by a combination of local brace deformation, brace buckling, and initial weld fracture in the gusset plates, with design criteria governed by the 20% maximum acceptance criteria for the mid-rise performance group (PG2).

Table 1 - Summary of functional recovery seismic performance factors for SCBF lateral systems up to 10 stories tall.

	FRC A/B/C			FRC D		
	R_{fr}	Δ_{afr}*	$R_{\mu f}$†	R_{fr}	Δ_{afr}*	$R_{\mu fr}$†
Analysis results	3.5	0.75%	1.15	4.0	0.75%	1.15
Judgment-based upper limit	4	1.25%	--	5	1.75%	--
Recommendation – SCBF	**3.5**	**0.75%**	**1.15**	**4.0**	**0.75%**	**1.15**

†*$R_{\mu fr}$ is only calculated for the recommended seismic performance factors*
**Drift checks are performed with Cdfr equal to Rfr for functional recovery design*

Contents

1. INTRODUCTION

This report documents the quantification of the functional recovery seismic performance factors for the special concentrically braced frame (SCBF) system. Quantification of the functional recovery seismic performance factors is performed in accordance with the proposed Section A.8.3.6 procedures of the 2026 National Earthquake Hazards Reduction Program (NEHRP) Provisions. The functional recovery seismic performance factors include the functional recovery response modification coefficient, R_{fr}, the functional recovery allowable story drift limit, Δ_{afr}, and the functional recovery structure ductility reduction factor, $R_{\mu fr}$. These are the equivalents of the response modification coefficient, R, the allowable story drift limit, Δ_a, and the structure ductility reduction factor, R_μ, used in ASCE/SEI 7 Chapters 12 and 13, but for design for functional recovery.

An archetype space of different building heights, designed with various functional recovery response modification coefficients and allowable drift limits, was developed. FEMA P-58/ATC-138 (FEMA, 2018a; ATC, 2021) models were then created. In accordance with the proposed Section A.8 procedures of the 2026 NEHRP Provisions, only structural components are included in these FEMA P-58/ATC-138 performance models. Design of the archetypes was performed using the automated design capability of SP3 (www.sp3risk.com) and engineering demand parameters (e.g., story drift ratios, peak floor accelerations, etc.) were estimated using SP3's Response Prediction Engine, which, while calibrated based on extensive nonlinear response history analyses, does not perform nonlinear response history analyses of the specific archetype directly.

Performance assessments of each model are conducted following FEMA P-58 (FEMA, 2018a) and ATC-138 recommendations to quantify the probability of safety-critical structural damage (P[SCSD]) for each archetype (Blowes et al., in press). The assigned safety class governs the triggering of SCSD for a given component and damage state according to the ATC-138 methodology. The safety class controls what percentage of components, in each story and direction, and for each independent structural system (i.e., gravity vs lateral) that can be in each damage state or greater, prior to triggering SCSD in the building. The P[SCSD] serves as an acceptable proxy for the probability of exceeding the target functional recovery times for structural-only models, as outlined in section CA.8.3.5 of the 2026 NEHRP Seismic Provisions.

The functional recovery seismic performance factors are selected such that archetypes designed for that R_{fr} and Δ_{afr} result in less than a 10% mean P[SCSD] in each performance group and less than 20% P[SCSD] for any individual archetype for Functional Recovery Category (FRC) A, B and C. The 10% and 20% thresholds are modified to 15% and 25%, respectively, for FRC D. These limits are in accordance with the proposed Section A.8.3.6 procedures of the 2026 NEHRP Provisions. All analyses are conducted at the Functional Recovery Earthquake (FRE_R) level shaking corresponding to a Seismic Design Category $D_{max,FRE}$ condition with two-point spectral ordinates S_{dsfr} and S_{d1fr} of 1.25g and 0.75g, respectively.

2. ANALYSIS METHODS

2.1. Design Iteration and Acceptance Criteria for Seismic Performance Factors

For each individual archetype, design iterations are carried out using values of R_{fr} and Δ_{afr} across the ranges of 1 through R (i.e., up to the response modification coefficient used in life-safety design) and 0.5% through 2.0% (i.e., up to the maximum allowable story drift ratio for Risk Category II structures), respectively. The response modification coefficient, R, is 6 for SCBF systems, in accordance with line B.2 of Table 12.2-1 of ASCE 7-22 (ASCE, 2022). These design iterations are performed using the SP3 design engine that estimates the strength and stiffness of each design to estimate appropriate structural responses and subsequent estimates of SCSD.

In each performance group, the combination of R_{fr} and Δ_{afr} is deemed to be acceptable if the mean P[SCSD] is less than 10%, and the maximum P[SCSD] across all archetypes in the performance group is less than 20% for quantifying the functional recovery seismic performance factors for Functional Recovery Category (FRC) A, B and C. For FRC D, the mean and maximum P[SCSD] across all archetypes in a performance group must be less than 15% and 25%, respectively. The recommended design values for a particular system are taken as the most restrictive across all performance groups, rounded to the nearest increment considered (0.25 for R_{fr} and 0.25% for Δ_{afr}).

The requirements of the proposed Section A.8.3.6 procedures of the 2026 NEHRP Provisions impose that R_{fr} and Δ_{afr} shall not be taken less than R/1.5 and 1.25% for FRC A, B and C and R/1.25 and 1.75% for FRC D. Additionally, to verify the strength and stiffness coupling inherent to each design variant, each archetype model is re-assessed under an independent strength and stiffness assumption, i.e., where additional strength prescribed by R_{fr} does not result in additional stiffness to the building. Analysis outcomes from the independent-strength-and-stiffness assessment are checked to ensure the maximum P[SCSD] does not exceed the acceptance criteria (20% for FRC A/B/C and 25% for FRC D), where applicable. The judgment-based upper limit and the independent-strength-and-stiffness check provide a reasonable limit that prevents excessive reliance on the analytical results and recognizes the historical precedent set by the higher Risk Categories.

2.1.1. Safety-Critical Structural Damage (SCSD)

The triggering of SCSD is governed by the assigned safety class of a given component and its damage state, according to the ATC-138 methodology (ATC, 2021). The safety class controls the percentage of components in each story and direction that can be in each damage state or greater before triggering SCSD. A summary of the ATC-138 safety class descriptions and acceptance thresholds is shown in Table 2.

Table 2. ATC-138 safety-class definitions for triggering SCSD (ATC, 2021).

Safety Class	Description	Acceptance Threshold[a]
0	Slight damage that is not a safety concern and will never trigger an unsafe placard	N/A
1	Moderate damage that may be visually concerning, but does not substantially reduce the lateral strength of the component.	50%
2	Severe damage that causes substantial loss of lateral strength of the component, but does not substantially reduce its vertical load-carrying capacity.	25%
3	Severe damage that compromises both the lateral and vertical load-carrying capacity of the component.	10%

[a] Percentages reflect the upper quantity of components, in each story and direction, that can be in a safety class of interest before triggering safety-critical structural damage (SCSD). The safety critical structural damage check is performed independently for each independent system in the building (e.g., the gravity vs. lateral system).

2.2. Fragility Functions for SCBFs

Fragility functions are used to relate structural responses to likely damage and consequences. Fragility functions are commonly modeled by a lognormal distribution defined by a lognormal mean (θ) and standard deviation (β). For a given structural component, sequential damage states (DSs) can be represented by individual fragility functions that describe the likelihood of a distinct level of damage and corresponding level of repair effort and consequences. Additionally, damage states may be mutually exclusive, with a single fragility function representing multiple outcomes (i.e., sub-damage states). Each likelihood is assigned a weighting that sums to unity (e.g., 0.25 + 0.75 = 1). The fragility functions used in the current study use both sequential and mutually exclusive damage state definitions. More general background information on fragility functions and damage state development can be found in FEMA P-58-1 (FEMA, 2018a).

The following sub-sections provide details on the structural component fragility functions, including:

- SCBF braced frame fragilities
- Bolted shear tab gravity connections
- Column base plates

Foundation elements are considered rugged in the current analysis. Fragility functions for foundation elements were not developed during the FEMA P-58 project, and foundation elements are specifically included in the list of acceptable rugged components in Appendix I of FEMA P-58-1 (FEMA, 2018a). Additionally, column splice connections for the special concentrically braced frame columns are assumed to be rugged based on the requirements in

AISC 341-22 Section F2.6 (AISC, 2022), which further references the requirements of Section D2.5.

2.2.1. SCBF Braced Frame Fragilities

The FEMA P-58 fragility database contains several steel brace fragility variants including those for special and ordinary concentric braced frames; wide flanged (WF), hollow structural section (HSS), and double angle brace type; chevron, X-braced, and single diagonal bracing configurations. The FEMA P-58 fragility functions for steel braces are based on a review of 69 experimental studies, mostly comprised of special concentrically braced frames, but also including some eccentrically braced frames, and buckling restrained braces (Roeder et al., 2009).

New experimental testing, funded by AISC and conducted within the last year, were used to develop new fragility functions for special concentrically braced frames (Sen and Mrema, 2025). These updated fragility functions are specific to specially detailed braced frames and reflect new compactness limits (b/t) currently under ballot for adoptions into the 2027 AISC Seismic Provisions. The current FEMA P-58 fragilities do not comply with these updated compactness limits. The braced frame fragilities are discretized for three bracing types: square HSS, round HSS, and WF. The new fragilities follow a similar four damage state structure as the FEMA P-58 fragilities and are widely applicable to various brace configurations (e.g., chevron vs X bracing, etc.). The updated SCBF brace fragility models are provided in Table 3 and are used in this study to quantify the recommended functional recovery seismic performance factors. Unlike the FEMA P-58 fragilities, damage states are only provided for one buckled state in relation to brace depth (opposed to several state in FEMA P-58) as there is insufficient experimental evidence to justify separate damage states for minor buckling in relation to brace depth.

The engineering demand parameter (EDP) used to develop the updated fragilities is *Story Drift Range*. Story drift range is the sum of the absolute magnitudes of drift in each direction of loading. For example, a system that undergoes a story drift range of 4% might have +2% and -2% peak drifts in each direction, or in another scenario, +1% and -3% drift. Axial deformation range of the brace is better correlated with its post-buckling damage states (such as fracture) than deformation in just one direction. This is because brace fracture occurs in tension but is strongly affected by strain accumulation in the brace plastic hinge region in compression. Compared to story drift, story drift range is a more reliable predictor of brace performance that precludes the need to distinguish between system configurations.

To convert from axial strain to story drift range for the purely axial experimental tests (without connecting frame components) it was assumed that:

- The only source of inelastic deformation in the system is brace axial deformation
- The brace is at a 45-degree angle.
- The brace length is 77% of the length between the brace work points.

The assumed 45-degree angle produces the highest axial strain per unit of drift. Therefore, damage occurs at slightly lower drift range thresholds than would be for other angles (i.e., this is a conservative assumption). The assumed brace length is based on the average from 26 frame sub-assembly tests.

Table 3. Updated Special concentric braced frame fragility functions in terms of story drift range.

Damage State	**Damage Description**	**Safety Class**[b]	**Brace Type**	**Median (θ)**[a]	**β**
DS1	Minor brace buckling > depth of the brace. Brace has not yet exhibited cracking or tension yielding.	0	Square HSS	0.52%	0.4
			Round HSS	0.61%	0.4
			WF	1.2%	0.4
DS2	Initiation of gusset plate weld fracture.[e]	1[d]	Square HSS	3.2%	0.2
			Round HSS	3.2%[c]	0.2
			WF	3.2%[c]	0.2
DS3	Initiation of brace local deformation, including local buckling of WF sections and cupping in HSS sections.	2	Square HSS	3.7%	0.33
			Round HSS	3.5%	0.26
			WF	5.3%	0.3
DS4	Complete brace fracture.	2[d]	Square HSS	5.3%	0.29
			Round HSS	5.4%	0.29
			WF	6.8%	0.3

[a] Fragility function is a lognormal distribution with median and standard deviation of θ and β, respectively. The EDP is story drift range. Story drift range is the sum of the absolute magnitudes of drift in each direction of loading and typically ranges from 1.5 to 2.0 times the peak story drift, as discussed in Section 2.4 below.

[b] SC 1 = 50%, SC 2 = 25%, SC 3 = 10% allowable quantity of damaged component per direction per story; SC 0 does not cause SCSD.

[c] For WF and Round HHS test, all experimental tests were conducted on axial brace test without frame assemblies. Therefore, the DS2 capacity is adopted from full sub assembly tests for square HSS.

[d] Additional studies were conducted where more consequential safety classes were assigned to DS2 and DS4, but it did not change the final recommendations.

[e] An example of gusset plate fracture initiation damage is shown in Figure 1.

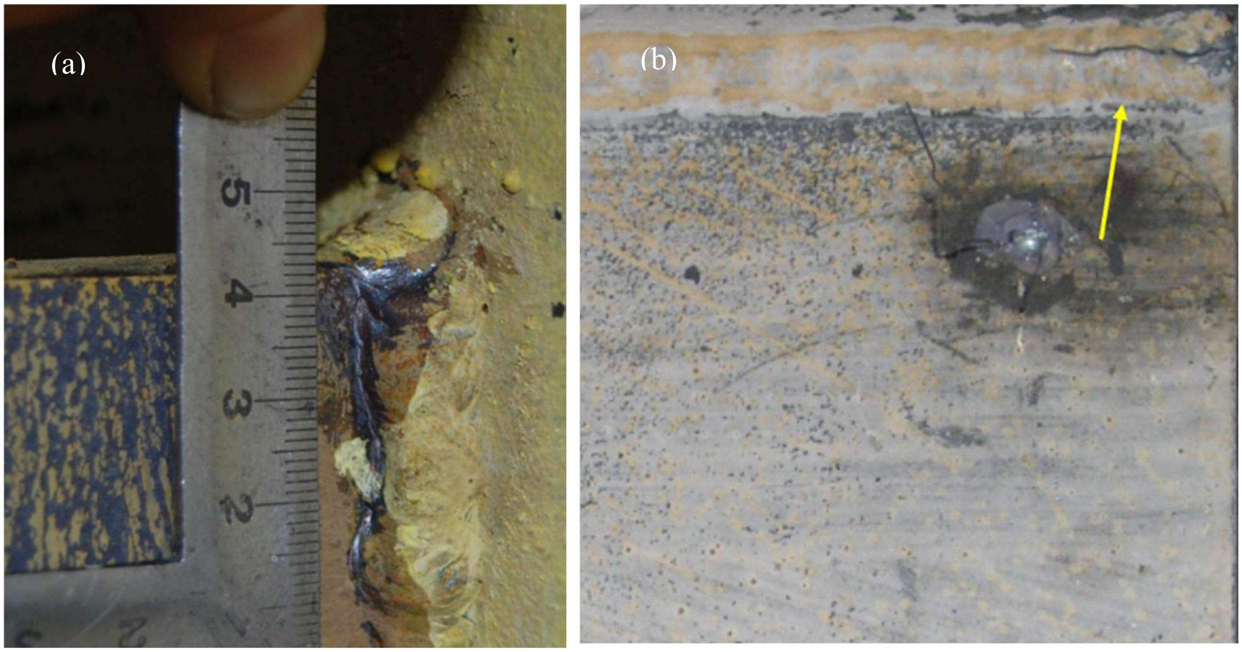

Figure 1 – Examples of DS2: initiation of gusset plate fracture, for (a) fillet welds (Sen, 2014) and (b) complete joint penetration welds (Herman, 2007).

2.2.2. Steel Gravity Connection Fragilities

Steel gravity beam-to-column connections are based on fragility development by Deierlein and Victorsson (2008) during the FEMA P-58 Project and are available within the FEMA P-58 fragility database. The fragilities are based on thirteen experimental tests on simple bolted shear tab connections conducted by Liu and Astaneh (2000). Fragilities are developed using story drift ratio as the EDP.

Fragility functions for steel gravity connections are comprised of three sequential damage states with DS1 split into two mutually exclusive DSs to either conduct or neglect minor repairs. DS2 is assigned a Safety Class of 2, while DS3 is assigned a Safety Class of 3. ATC-138 assigned Safety Class 2 to both DS2 and DS3. Following review of the damage description for DS3, the Safety Class was increased to 3 to be more in line with the Safety Class definitions (see Table 2) based on the judgment of the peer review committee. A summary of the fragility functions and corresponding safety class assignments is provided in

Table 4. Figure 2 shows example photographs of each damage state. A plot of the fragility functions is provided in Figure 3.

Table 4. Bolted shear tab gravity connection fragility damage states and corresponding safety classes.

Damage State[a]	Median (θ)[b]	β	Safety Class[c]	Damage Description	Repair Measures
DS1a (0.95)	4.0%	0.4	0	Yielding of shear tab and elongation of bolt holes, possible crack initiation around bolt holes or at shear tab weld. Damage in field is either obscured or deemed to not warrant repair. No repair conducted.	Field condition is deemed to not warrant repair by field observation.
DS1b (0.05)	4.0%	0.4	0	Yielding of shear tab and elongation of bolt holes, possible crack initiation around bolt holes or at shear tab weld.	Careful inspection and welded repair to any cracks and possible replacement of shear tab if bolt hole deformations are excessive (possible for 6-bolt or deeper shear tabs).
DS2	8.0%	0.4	2	Partial tearing of shear tab and possibility of bolt shear failure (6-bolt or deeper connections).	Repairs will include either welded repair of shear tab or possible complete replacement of shear tab and installation of new bolts. Repairs may require shoring of beam.
DS3	11.0%	0.4	3[d]	Complete separation of shear tab, close to complete loss of vertical load resistance.	Repair will include complete replacement of shear tab and installation of new bolts. Repairs will require shoring of beam.

[a] Mutually exclusive damage states (e.g., DSXa and DSXb) include the probability of occurrence in parentheses

[b] Fragility function is a lognormal distribution with median and standard deviation of θ and β, respectively. The EDP is story drift ratio.

[c] SC 1 = 50%, SC 2 = 25%, SC 3 = 10% allowable quantity of damaged components per direction per story; SC 0 does not result in SCSD.

[d] This assessment deviates from the ATC 138 assignment of DS3 as Safety Class 2 based a review of the safety class definitions and the judgment of the authors. This change leads to more conservative results.

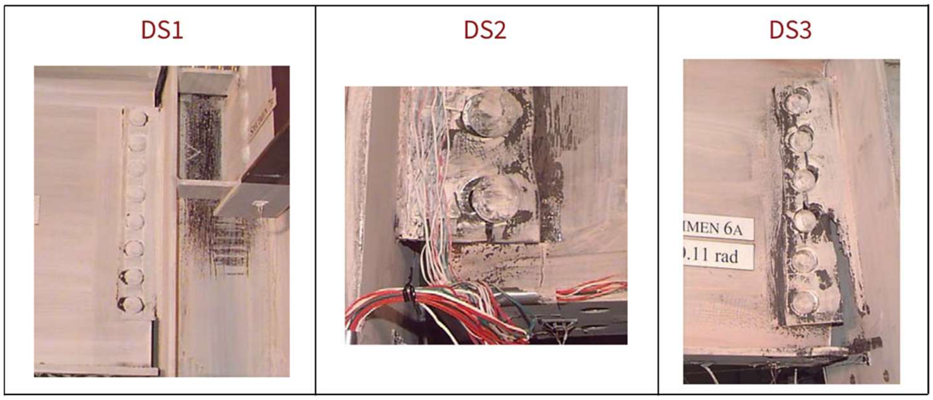

Figure 2 – Illustration of damage states for steel shear tab connections (Deierlein and Victorsson, 2008).

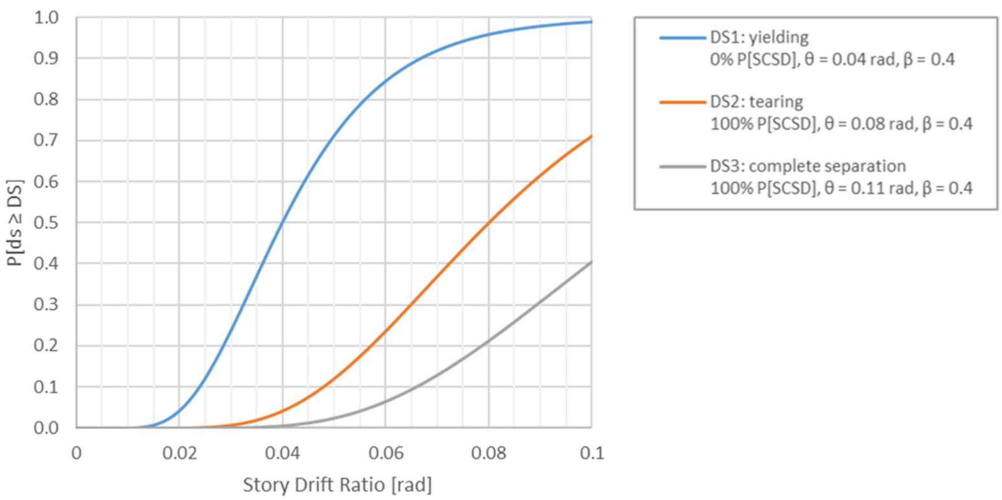

Figure 3 – Fragility functions for bolted shear tab gravity connections.

2.2.3. Steel Column Baseplate Fragilities

Steel column baseplates fragilities were developed by Deierlein and Victorsson (2008) during the FEMA P-58 Project and are available within the FEMA P-58 fragility database. The fragilities are based on thirteen experimental tests on exposed column baseplates reported by three studies (Burda and Itani, 1999; Fahmy, 1999; Hajjar et al. 2005). All tests considered loading in the strong axis direction of the column. Fragilities are developed using story drift ratio as the EDP.

Fragility functions for steel column baseplate connections are comprised of three sequential damage states with DS1 split into two mutually exclusive DSs to either conduct or neglect minor repairs. DS2 is associated with crack propagation into the column or baseplate. DS3 represents the complete fracture and dislocation of the column. DS2 and DS3 are assigned Safety Classes of 2 and 3, respectively. A summary of the fragility functions is provided in Table 5.

Table 5. Steel column baseplate connection fragility damage states and corresponding safety classes.

Damage State[a]	Median (θ)[b]	β	Safety Class[c]	Damage Description	Repair Measures
DS1a (0.95)	4.00%	0.4	0	Initiation of crack at the fusion line between the column flange and the base plate weld. Damage in field is either obscured or deemed to not warrant repair.	Field condition is deemed to not warrant repair by field observation.
DS1b (0.05)	4.00%	0.4	0	Initiation of crack at the fusion line between the column flange and the base plate weld.	The repair will involve removal of a portion of grade slab, gouging out material surrounding the fracture initiating and re-welding, then repair of slab.
DS2	7.00%	0.4	2	Propagation of brittle crack into column and/or base plate.	Depending on the crack trajectory, the repair will range from replacement of a portion of the column or base plate to full replacement of the column base. Replacement will require shoring of column, torch cutting to remove damaged material, and fabrication and field welding to install replacement material.
DS3	10.00%	0.4	3	Complete fracture of the column (or column weld) and dislocation of column relative to the base.	Repair would likely involve replacing the entire base plate assembly and most of the column in the story above the base plate.

[a] Mutually exclusive damage states (e.g., DSXa and DSXb) include the probability of occurrence in parentheses
[b] Fragility function is a lognormal distribution with median and standard deviation of θ and β, respectively. The EDP is story drift ratio.
[c] SC 1 = 50%, SC 2 = 25%, SC 3 = 10% allowable quantity of damaged components per direction per story; SC 0 does not result in SCSD.

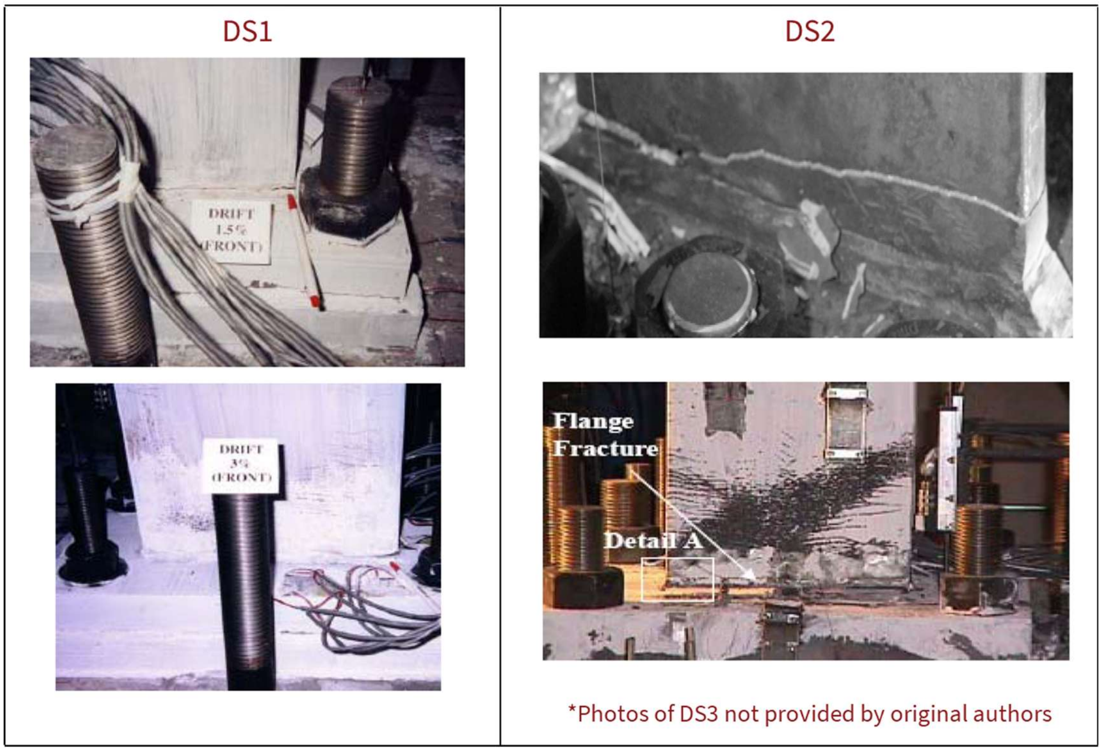

Figure 4 – Illustration of the first two damage states for steel column baseplates (Deierlein and Victorsson, 2008).

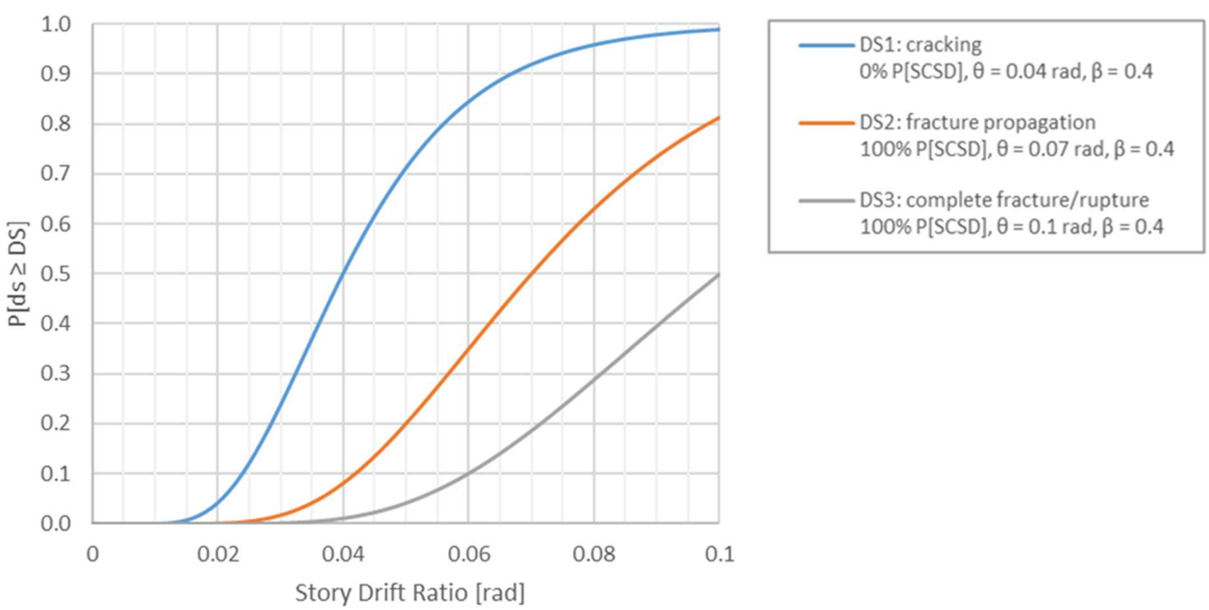

Figure 5 – Fragility functions for steel column baseplates.

2.3. Archetypes Considered for Analysis

To determine the combination of R_{fr} and Δ_{afr} that results in acceptable functional recovery performance, an archetype space is divided into performance groups, analyzed, and the overall parameters are determined by the worst-case performance group. This is similar to the FEMA P-695 methodology used for quantifying performance factors for life-safety (FEMA, 2009) and is in accordance with the proposed procedures in Section A.8 of the 2026 NEHRP Provisions.

The SCBF system has an archetype space comprised of two different performance groups and a total of 12 individual archetype variants. The background on the development of the archetype design space is presented in the following sub-sections.

2.3.1. Building Configuration and Structural Component Population

All archetypes assume a constant plan area of 100 feet by 100 feet. Story heights are assumed to be 16 and 14 feet for the first and typical stories, respectively. The following archetype variables are considered:

- Number of stories.
- Bracing Types.

Building heights range from 2 to 10 stories, split into two height classes: low-rise (2, 3, and 4 stories) and mid-rise (6, 8, and 10 stories). High-rise (12, 16, and 20 stories) buildings are to be considered in a later study. SCBF bays are configured in a chevron pattern up the building height, with braced bay lengths of 30 feet, with one braced bay on each side of the building. Typical plan and elevation layouts, along with populated structural components, are shown in Figure 6. Steel shear tab gravity connections are assumed at all locations outside the SCBFs. Column base plates are populated at each base column within an SCBF bay.

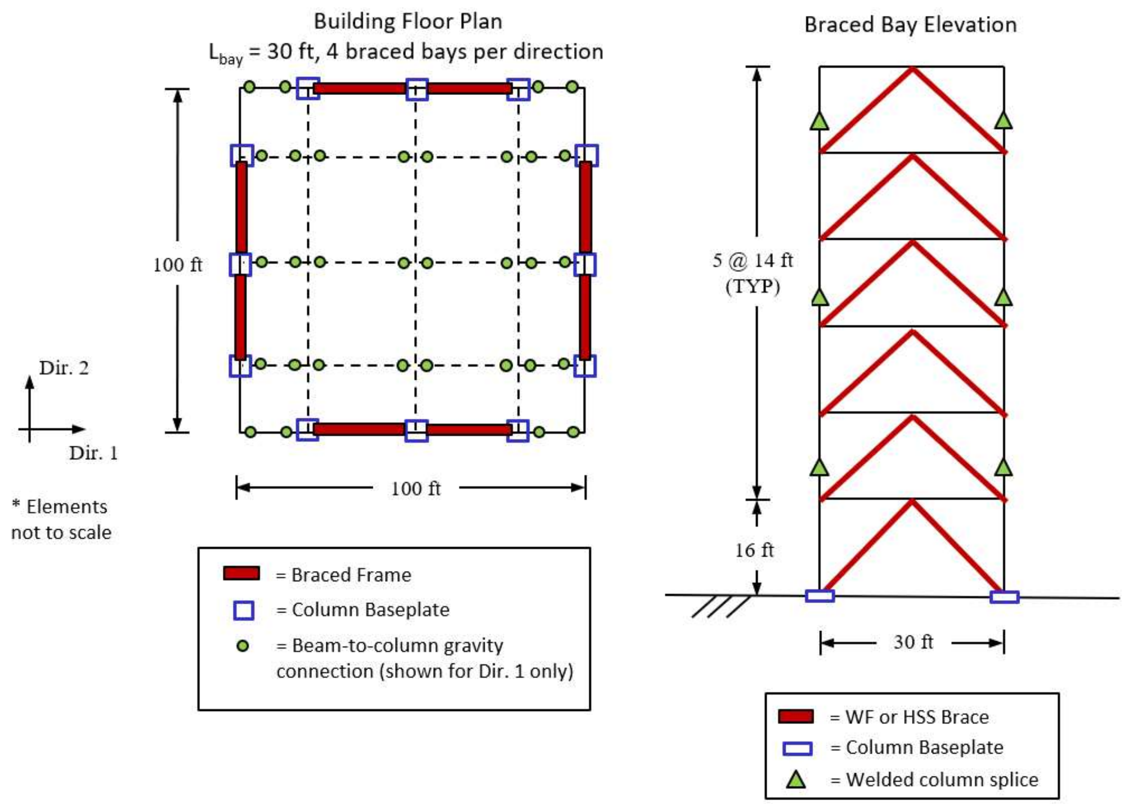

Figure 6 – Illustration of (a) plan layout and (b) braced frame bay elevation for SCBF archetypes, showing the typical population of structural components.

2.3.2. Performance Groups for SCBF

Performance groups are delineated based on building characteristics that influence the structural properties and global response of SCBF buildings. The performance group heights considered were low-rise (PG1) and mid-rise (PG2). The use of building height to define (or delineate) performance groups has a strong precedence in numerous applications of the FEMA P-695 methodology, which serves as a basis of the performance group concept used in the current study and underlying NEHRP Appendix A provisions. As a minimum, performance groups are distinguished between short-period (short structures) and long-period (tall structures). Additionally, the bracing types were varied within each performance group, which affect the component fragilities and estimated structural properties of each archetype. The definition of each performance group is shown in Table 6.

Table 6. Summary of SCBF performance groups.

Performance Group	Stories	Brace Types
PG1a	2, 3, 4	WF
PG1b		Square HSS
PG1c		Round HSS
PG2a	6, 8, 10	WF
PG2b		Square HSS
PG2c		Round HSS

2.4. Estimation of Structural Responses

The structural responses for the archetypes were determined using the SP3 Structural Response Prediction Engine (SRPE) (Cook et al. 2018). The SRPE generates a simplified linear multi-degree-of-freedom model representative of strength and stiffness requirements. Nonlinear response is determined by modal analysis, which is then modified to account for the nonlinear behavior of the system. The expected nonlinear behavior is calibrated by sampling from Incremental Dynamic Analysis (IDA: Vamvatsikos and Cornell, 2002) results from high-fidelity nonlinear structural models.

The following sections provide an overview of the analytical basis behind the SRPE and the quantification of different Engineering Demand Parameters (EDPs). This section focuses on the prediction of median response conditioned on spectral acceleration (Sa). Record-to-record uncertainty and modeling uncertainty are modeled according to FEMA P-58 (FEMA, 2018b).

2.4.1. Analytical Basis Behind the SCBF SRPE in SP3

The SRPE braced-frame submodule is used for the estimation of structural responses for SCBF systems performed in this assessment. The SRPE sub-module for concentrically braced frames was developed the nonlinear response-history analyses of 16 SCBF archetype models, all complying with the seismic design provisions of ASCE/SEI 7-22 (Sen and Mrema, 2025). The 16 archetype buildings were modeled as planar frame lines using OpenSees (McKenna et al. 2010), but were modeled in 3D to capture out-of-plane failure modes in fiber elements. Braces were modelled as inelastic fiber section elements with initial imperfections to properly induce buckling, and all other elements were modeled as elastic.

In calibrating the SRPE responses for SCBF systems, the system response and nonlinear localizations estimates are developed by accounting for differences in model periods, mode shapes, overstrength, and ductility capacity, thus ensuring the generalizability of the response estimation beyond the SCBF buildings originally studied. In the elastic range, the SCBF system has similar mode shapes to the buckling-restrained brace frame system. However, stiffness, ultimate strength, ductility capacity, failure modes, nonlinear degradation, and drift localization differ between the two lateral systems. There were no significant differences in the responses across the bracing configuration variants, so no distinction was made in the SRPE.

Braced frame bays were modelled in two configurations: chevron and multi-story X-bracing (i.e., alternating chevron bracing). Both WF and HSS braces were considered. Brace sections are sized and detailed to comply with the requirements of ANSI/AISC 341-22 (AISC, 2022). All archetypes were designed to be regular in plan, 2 to 9 stories tall, with 14 ft story heights over a 16 ft first story. The layout and configuration of the models used to develop the SCBF SPRE are similar to, but not identical with, the models previously used at NIST (2010), which were designed to comply with an older version of the seismic design provisions. A summary of the different archetype buildings considered for SRPE calibration of SCBFs is provided in Table 7.

All models were analyzed using the FEMA P-695 far-field ground-motion set (FEMA, 2009), which consists of 44 ground motions (i.e., 22 horizontal pairs). Incremental Dynamic Analysis (IDA: Vamvatsikos and Cornell, 2002) was used to obtain a range of linear and nonlinear structural responses for calibration. The key EDP for predicting structural response in the SCBF system is the peak story drift range used to estimate SCSD. An overview of the estimation of this EDP is discussed in the following sub-sections.

Table 7. Summary of building models used for calibration of the SCBF SRPE.

ID	No. Stories	Brace Configuration	Brace Type
201	2	Chevron	WF
202	2	Chevron	HSS
211	2	X-brace*	WF
212	2	X-brace*	HSS
301	3	Chevron	WF
302	3	Chevron	HSS
311	3	X-brace*	WF
312	3	X-brace*	HSS
601	6	Chevron	WF
602	6	Chevron	HSS
611	6	X-brace*	WF
612	6	X-brace*	HSS
901	9	Chevron	WF
902	9	Chevron	HSS
911	9	X-brace*	WF
912	9	X-brace*	HSS

*X-bracing occurs over two stories (i.e., alternating chevron bracing)

2.4.2. *Structural Properties Estimation*

Building structural properties are estimated using a linear building model, with strength and stiffness scaled to meet corresponding design requirements. Typical levels of overstrength (e.g., due to expected material properties, etc.) are added after design requirements are satisfied, to provide the best possible estimate of the true strength and stiffness of the LFRS. The commercial version of SP3 also includes additional strength and stiffness contributions from the gravity system and nonstructural components, but these are excluded in this study for compliance with the procedures of Section A.8 of the 2026 NEHRP Provisions.

The process begins by determining the design parameters, including spectral values, response modification factor (R), deflection amplification factor (C_d), and related values (e.g., I_e). Next, a target seismic design drift is selected. For drift-controlled systems, such as most moment frames, this target is typically the design drift limit—for example, 2% for risk category II buildings. For strength-controlled systems, the target drift is a realistic value appropriate for the system type and building height; the expected design drift values are based on a database of hundreds of building designs (from archetype buildings in the SP3 SRPE database). Resilient design iterations use the same process with pairs of R_{fr} and Δ_{afr} for a given analysis. Notably, the deflection amplification factor for functional recovery (C_{dfr}) is taken equal to R_{fr}, and the building importance factor (I_e) is taken as unity per Section A.8 of the 2026 NEHRP Provisions.

Following this, the period of a representative design model (limited to the LFRS) is determined, considering the target seismic drift and stability requirements (ASCE 7-22 Section 12.8.7). This involves constructing a simple multi-degree-of-freedom (MDOF) model that reflects the system's mass and stiffness characteristics. For instance, moment frames tend to be more shear-dominated, whereas walls and braced frames are more flexure-dominated. This approach is based on a method developed by Miranda (1999) and Miranda and Reyes (2002) but utilizes matrix structural analysis with mass and stiffness matrices rather than purely analytical equations; it also incorporates the ability to model rotational flexibility at the base.

Starting from a very low stiffness, the stiffness matrix is systematically scaled (i.e., increased) until the model achieves the target drift or less while satisfying stability requirements. Generally, modal response spectrum analysis (MRSA) is used to generate structural properties for modern code-compliant buildings that are taller than four stories and located in high- or very high-seismic areas. For other cases, the equivalent lateral force (ELF) procedure is used. Wind drift checks can be included in this step but were omitted for this study.

Next, the expected strength and stiffness of the LFRS are determined, accounting for overstrength. These properties vary depending on the LFRS type and building height and are calibrated using results from OpenSees models and engineering judgment. For SCBF models, the HSS brace variants have a slightly higher overstrength than the WF braced variants due to the lack of available HSS sections that meet the ductility requirements, forcing designers to use larger sections than required in many cases. An additional optional check can be performed to ensure compatibility between strength and stiffness, where the stiffness is adjusted if it is too high or low in relation to the strength and yield drift.

The final estimates of the first three periods and mode shapes of the building are determined by performing an eigen analysis with the stiffness matrix and mass matrix. The final estimate of the ultimate base shear strength is determined from design strength and the expected overstrength.

2.4.3. Story Drift Ratio

The SCBF SRPE estimates peak story drift ratio at each story, accounting for the first three mode shapes and periods of the building and its peak strength. The peak roof drift ratio is estimated using a method that is similar to the ASCE 41 target roof displacement (ASCE, 2023; Section 7.4.3.3.2), but with factors calibrated directly from the OpenSees model results. The roof drift ratio depends on the fundamental building period, modal participation factor, spectral acceleration, and correction factors for nonlinear behavior. Next, a linear modal analysis is performed using the first three modes, and the results are scaled to the estimated roof drift. If the spectral acceleration demand is large enough to yield the structure, the story drifts are adjusted to account for nonlinear demands. Nonlinear demands are adjusted using an intensity factor S = Sa/(Vmax/W), where Sa is the first-mode spectral acceleration and (Vmax/W) denotes the normalized peak strength of the building based on expected properties. Larger values of S (i.e., more damage) result in more drift concentration in the lower stories. The way in which drifts localize as S increases is calibrated to nonlinear modeling results and depends on the building height (i.e., number of stories). An example calibration for a 12-story RC special moment frame model is shown in Figure 7. The solid lines represent the median peak drift profile from nonlinear time history analysis (NRHA) compared to SRPE response shown in thicker dashed lines. The dotted lines show the elastic response profile before adjusting for nonlinear behavior.

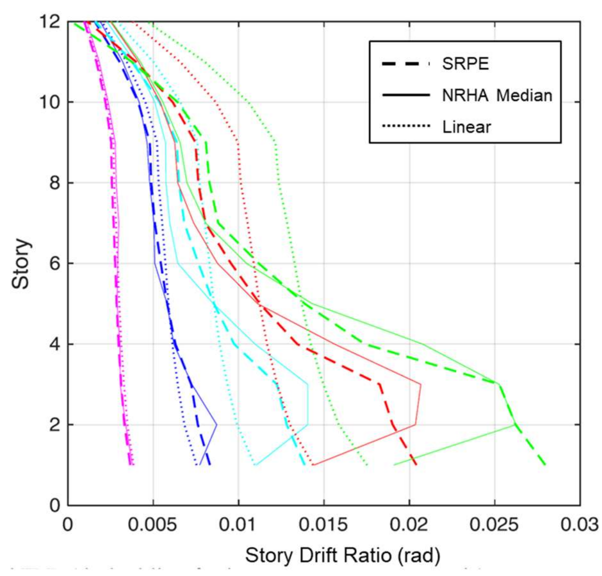

Figure 7. Comparison of SRPE (dashed) and median NRHA (solid) story drift ratio response for a 12-story RC special moment frame. Note, dotted lines represent predicted linear response prior to adjustment for nonlinear behavior. Figure adapted from Cook et al. (2018).

2.4.4. *Racking Story Drift Ratio*

In taller SCBF structures, a significant portion of the upper-story drift can result from column axial flexibility; specifically, axial elongation and shortening of the vertical members over the height of the building. Therefore, the total story drift can be decomposed into two components: a floor rotational component from column axial flexibility, and a racking component from in-plane deformation of the braced bay. Since only the racking deformation directly contributes to brace strain demand, this component is used in the analysis as the drift demand parameter brace fragilities. The relationship between total, rotational, and racking drifts is defined as:

$$\Delta_{total} = \Delta_{rot} + \Delta_{racking}$$

The total drift is calibrated as discussed in the previous section. The racking portion is obtained by subtracting an approximate rotational drift from the total drift. Rotational drift is straightforward to approximate because it's an elastic mechanism, since the columns are capacity-designed. The rotational drift ranges from 0 at the first story (since there is no vertical ground deformation considered in the analysis) to a peak value at the topmost level. For reference, the top story Δ_{rot} is approximately 0.2% for a 6-story model and 0.3% for 9-story models once the braces begin to yield and buckle.

2.4.5. *Story Drift Ratio Range*

As discussed in Section 2.2.1, the brace damage is best fit to the range of drift rather than just the peak drift. The story drift range is the maximum drift minus the minimum drift. For example, if the model experiences a maximum drift of 1.5% and a minimum drift of -2.4%, the peak story drift would be 2.4%, but the story drift range would be 3.9%, calculated as:

$$\Delta_{range} = \Delta_{max} - \Delta_{min} = 1.5\% - (-2.4\%) = 3.9\%$$

The story drift range (racking component of the story drift range) is approximated from the peak drift as a multiplier (between 1 and 2) of the peak story drift ratio (racking component), as illustrated in Figure 8.

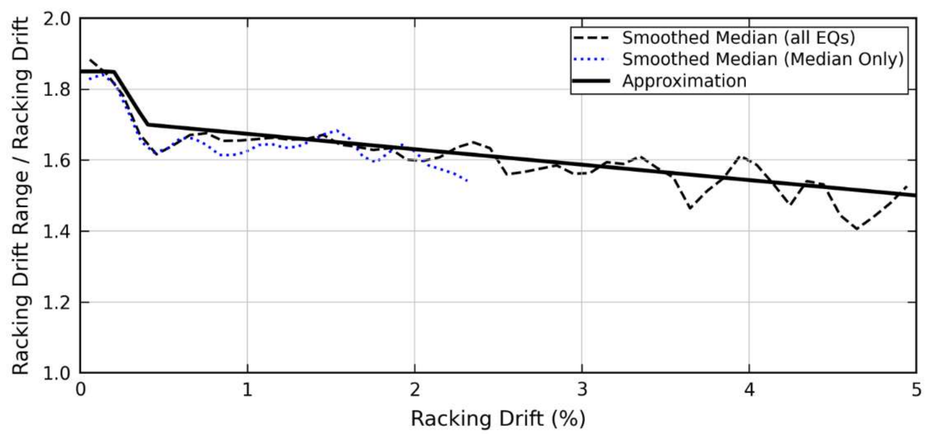

Figure 8. Approximate ratio of racking drift range to peak racking drift (solid) compared to the RHA results for all earthquake realizations (dashed) and median racking drift profile (dotted).

2.4.6. *Peak Floor Acceleration*

Peak floor acceleration (PFA) is computed based on spectral acceleration, building strength, and the first three modal periods and shapes of the building. First, elastic PFA is computed with modal time-history analysis using the FEMA P-695 far-field record set scaled to the intensity of interest. Then, if the spectral acceleration demand is large enough to cause yielding, PFA is adjusted using the intensity factor $S = S_a/(V_{max}/W)$. The amount of reduction of the response depends on how high the story is above the ground, because damage in the lower stories "isolates" the upper stories from acceleration input. An example calibration for a 12-story RC special moment frame model is shown in Figure 9. The solid lines represent the median PFA profile from NRHA compared to the SRPE response shown in thicker dashed lines. The dotted lines show the elastic response profile before adjusting for nonlinear behavior. Note that the largest intensity shaking (green lines) has significant reductions in PFA at upper stories due to damage in the lower stories.

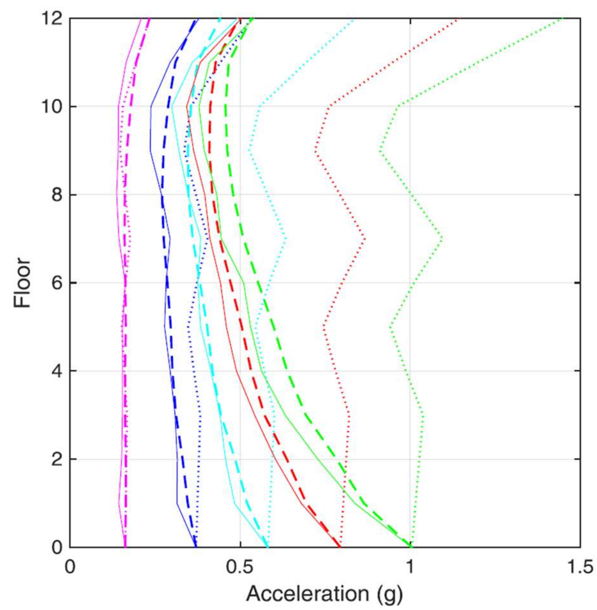

Figure 9. Comparison of SRPE (dashed) and median NRHA (solid) peak floor acceleration response for a 12-story RC special moment frame. Dotted lines represent predicted linear response before adjustment for nonlinear behavior. Figure adapted from Cook et al. (2018).

2.4.7. *Treatment of Residual Drift Ratio*

The FEMA P-58 residual drift model was updated during the ATC-138 project (ATC, 2021) and resulted in a supplemental FEMA P-58 background document *BD 3.7.26: Updated Model and Criteria for Residual Drift* (DeBock et al. 2024). The revisions to the original FEMA P-58 model allowed for distinctions between structural systems, based on recent analytical studies (Almeter et al. 2018; Vouvakis Manousakis et al. 2024).

The median residual story drift ratio (Δ_r) is estimated from the median transient story drift ratio (Δ) and yield drift ratio (Δ_y). The general format for simplified residual drift estimation has a trilinear form with a transition slope and a primary slope. The initial slope represents the elastic response range (i.e., $\Delta \leq \Delta_y$) where residual displacement is not expected. The transition slope reduces the rate of residual drift accumulation in the region just beyond elastic response to a specified drift ductility, after which, the steeper primary slope accumulates residual drift at a faster rate as peak drift demands increase. The end of the transition region is defined by a system specific drift value Δ_{shift}. An illustration of the basic components of the trilinear residual drift model is shown in Figure 10.

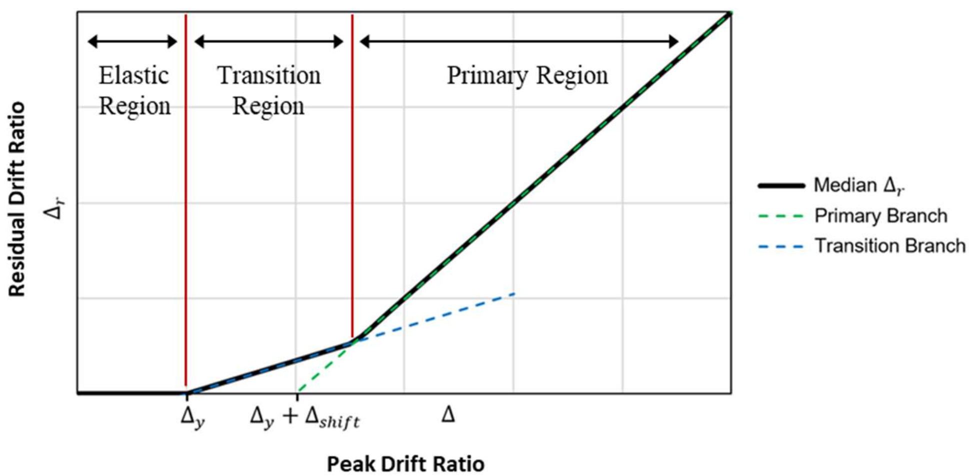

Figure 10 – Basic components of the trilinear model to estimate residual story drift as a function of peak story drift demand and yield story drift.

Three residual drift models were developed as part of the FEMA P-58 revisions, with parameters summarized in Table 8. For the SCBF system, the generalized inelastic residual drift model is selected according to the FEMA P-58 recommendations, as listed in Table 9. The recommended yield drift ratio (Δ_y) for SCBF systems is 0.3%. The residual story drift ratio as a function of story drift ratio demand for the SCBF system is shown in Figure 11.

Table 8. Parameters of updated FEMA P-58 residual drift models

Residual Drift Model	**Δ_{shift}**	**Primary Slope (a)**	**Transition Slope (b)**
Steel MRF	0.005	0.5	0.2
Steel BRBF	0.007	0.4	0.1
General Inelastic	0.008	0.35	0.15

Table 9. Recommended yield story drift ratio (Δ_y) and residual drift models by LFRS

LFRS	Δ_y (rad)	Residual Drift Model
Steel MRF	0.01	Steel MRF
Steel CBF	0.003	General Inelastic
Steel EBF	0.005	BRBF
Steel BRBF	0.002	BRBF
RC MF	0.0075	General Inelastic
RC Wall	0.0025	General Inelastic
Masonry	0.0025	General Inelastic
Wood or CFS light frame	0.075	General Inelastic

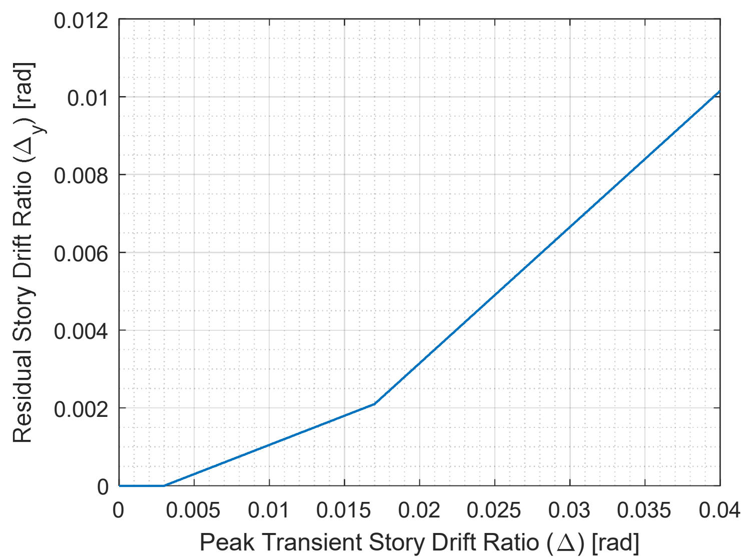

Figure 11. Residual drift model for the SCBF structural system, based on the general inelastic drift model and a 0.3% yield drift.

3. RESULTS

The tables and plots below show the R_{fr} and Δ_{afr} envelopes for each performance group variant combination. This design envelope identifies the possible design value combinations where all performance groups satisfy both the max and mean analysis criteria. Results are provided separately for both FRC A/B/C acceptance criteria in Section 3.1 and FRC D acceptance criteria in Section 3.2. Additional figures that illustrate general system performance in terms of structural response, controlling component damage, and controlling design features are provided in Section 3.3. Full details on the performance of individual archetypes are provided in the attached supplementary materials.

3.1. FRC A/B/C Analysis Results

Table 10 – R_{fr} values across various allowable drift limits required to satisfy the FRC A/B/C structural performance acceptance criteria for each performance group. Analysis results assume increased strength requirements impact building stiffness.

Performance Group	Criteria	Δ_{afr} 0.005	0.0075	0.01	0.0125	0.015	0.0175	0.02
PG1-SCBF	Max[1]	6	3.5	3.5	3.5	3.5	3.5	3.5
PG2-SCBF		6	3.5	2.5	2.5	2.5	2.5	2.5
PG1-SCBF	Mean[1]	6	3.5	3.5	3.5	3.5	3.5	3.5
PG2-SCBF		6	3.5	3	3	3	3	3
	Envelope	6	3.5	2.5	2.5	2.5	2.5	2.5

[1]In each performance group, the combination of R_{fr} and Δ_{afr} is deemed to be acceptable if the mean P[SCSD] is less than 10%, and the maximum P[SCSD] across all archetypes in the performance group is less than 20%.

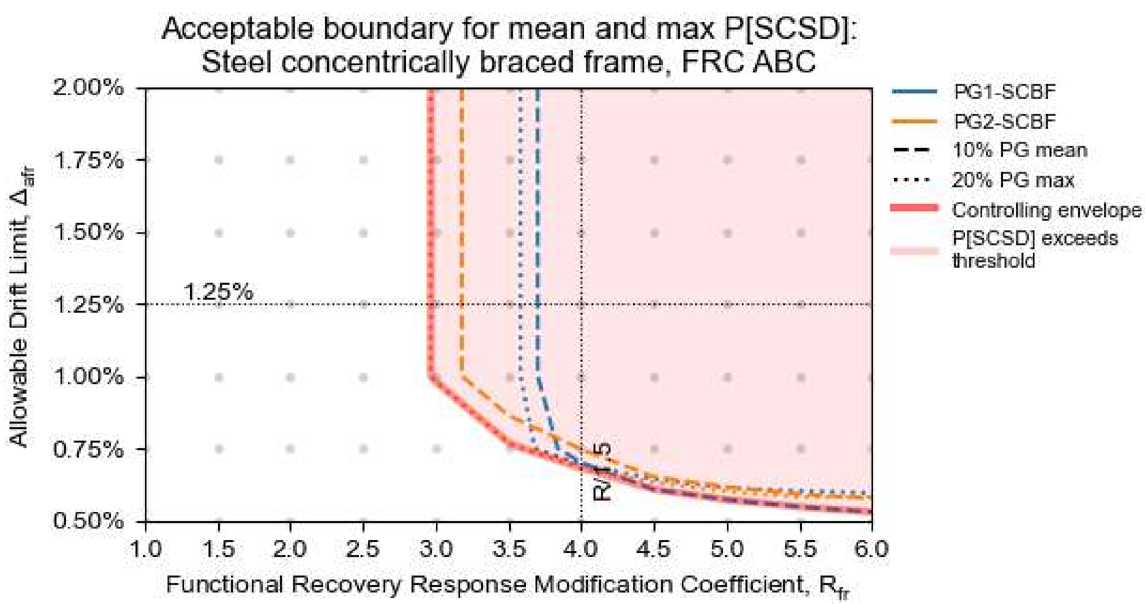

Figure 12 – Combination of R_{fr} and Δ_{afr} values required to satisfy the FRC A/B/C structural performance acceptance criteria for each performance group. Analysis results assume increased strength requirements impact building stiffness.

3.2. FRC D Analysis Results

Table 11 – R_{fr} values across various allowable drift limits required to satisfy the FRC D structural performance acceptance criteria for each performance group. Analysis results assume increased strength requirements impact building stiffness.

Performance Group	Criteria	Δ_{afr} 0.005	0.0075	0.01	0.0125	0.015	0.0175	0.02
PG1-SCBF	Max[1]	6	4	3.5	3.5	3.5	3.5	3.5
PG2-SCBF		6	3.5*	3	3	3	3	3
PG1-SCBF	Mean[1]	6	4	3.5	3.5	3.5	3.5	3.5
PG2-SCBF		6	4.5	3	3	3	3	3
	Envelope	6	3.5*	3	3	3	3	3

[1]In each performance group, the combination of R_{fr} and Δ_{afr} is deemed to be acceptable if the mean P[SCSD] is less than 15%, and the maximum P[SCSD] across all archetypes in the performance group is less than 25%.

*The final selected R_{fr} is higher than the allowable value indicated on this table. However, the selected R_{fr} and Δ_{afr} combination results in a P[SCSD] value that exceeds the acceptance criteria by a justifiably small margin (<2%). Please see Figure 13, which shows that the final selected combination is close to the envelope.

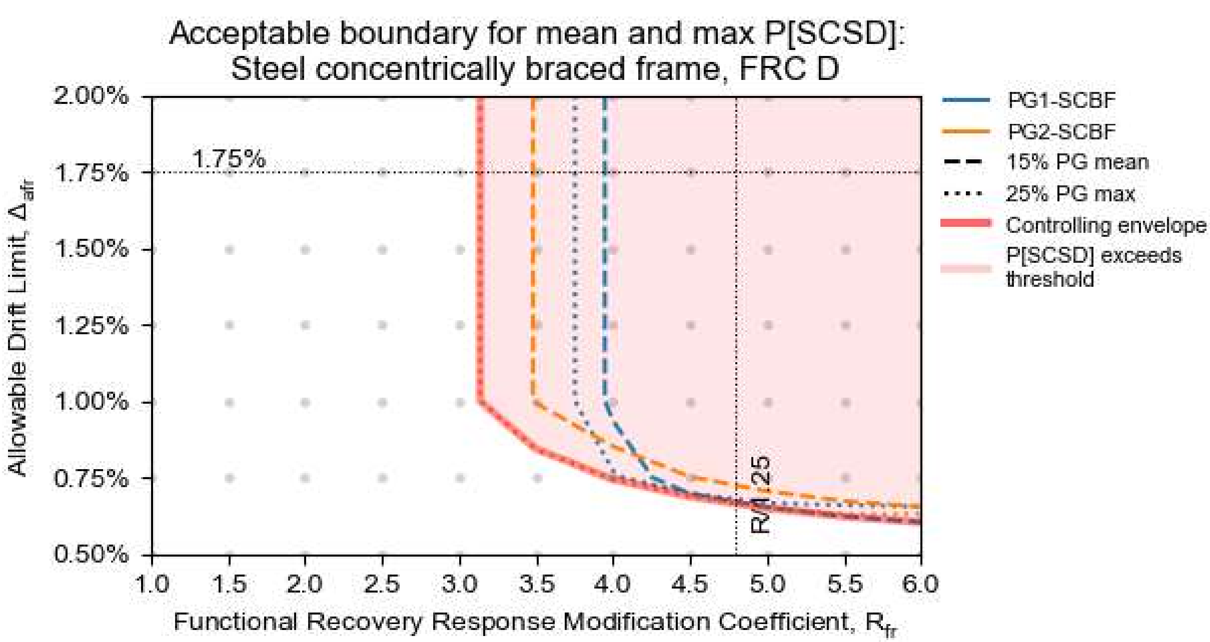

Figure 13 – Combination of R_{fr} and Δ_{afr} values required to satisfy the FRC D structural performance acceptance criteria for each performance group. Analysis results assume increased strength requirements impact building stiffness.

3.3. System Response

The figures below provide detailed insights into the general response and performance outcomes of the models making up each performance group. Figure 14 shows how design drift (Δ_{afr}) relates to median realized drift (x-axis), and how realized drift relates to P[SCSD] (y-axis). The median realized drift is the median peak story drift, in a given story, from all the realizations of peak story drift (~2,000) simulated as part of the FEMA P-58 Monte Carlo assessment. Figure 15 and Figure 16 further break down the contributions of SCSD by structural component type, and shows that brace component SCSD is dominant in many of the performance results for SCBF buildings. All results presented in this section are general to the response of the system and not specific to Functional Recovery Category.

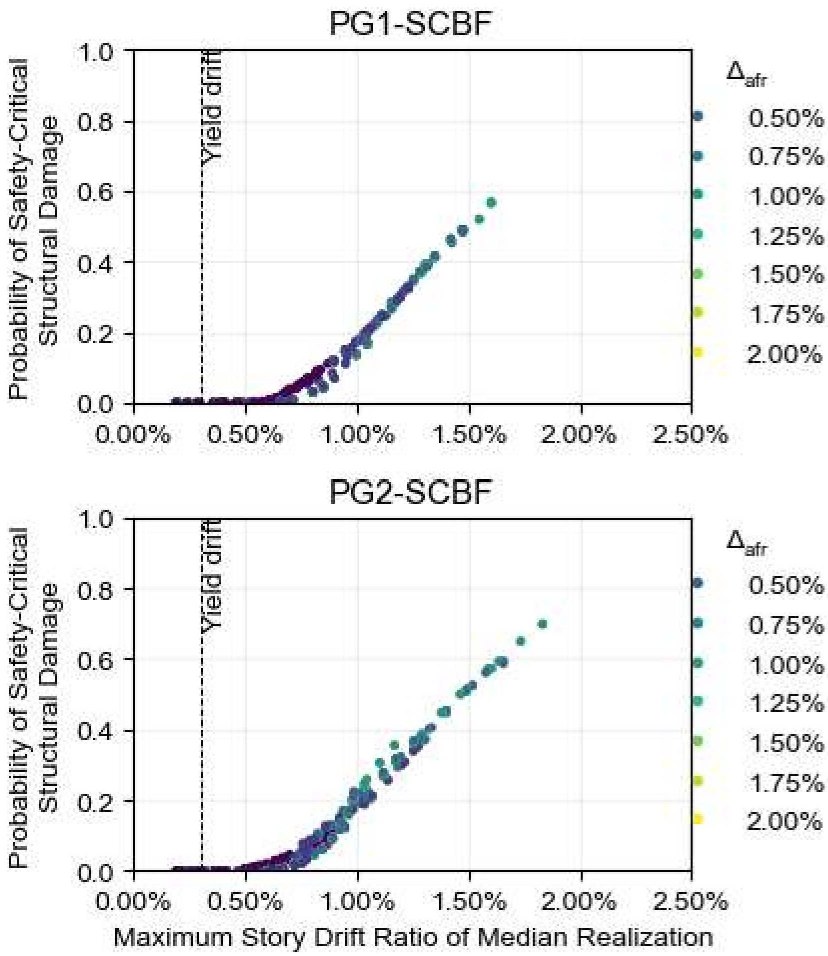

Figure 14 - Relationship between peak realized drift (median) and P[SCSD] for all archetypes.

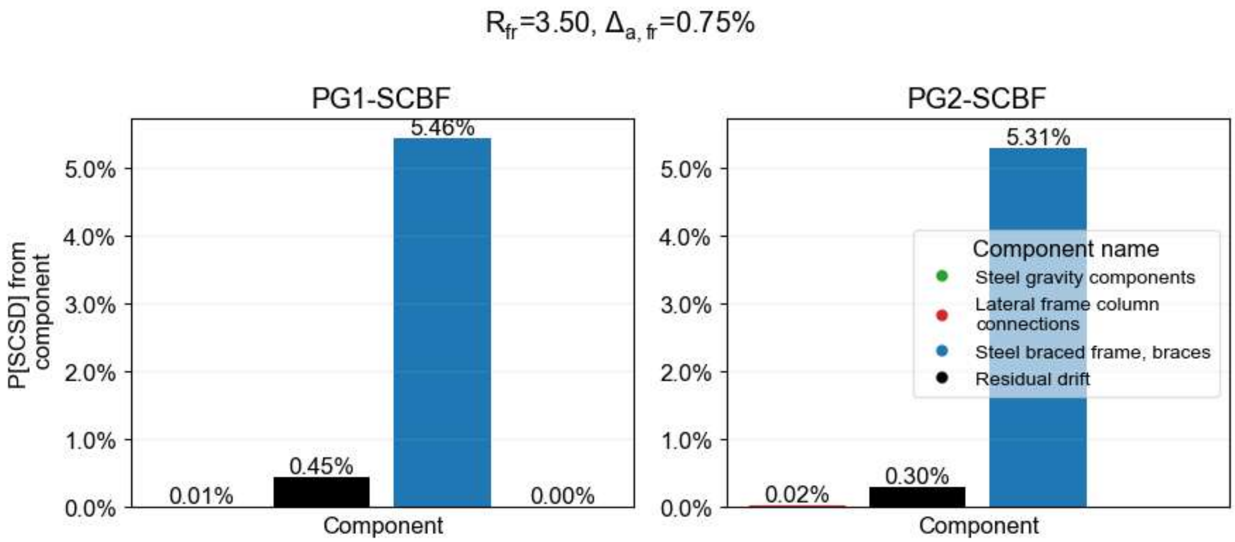

Figure 15 – Component damage contribution to P[SCSD] for each performance group at the recommended design points for FRC ABC.

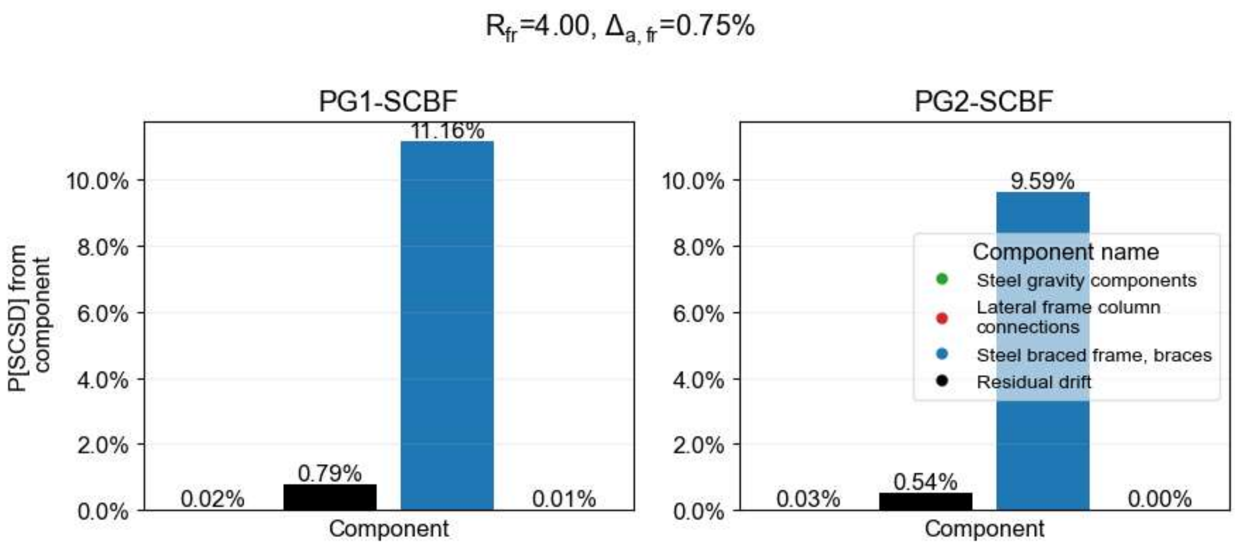

Figure 16 – Component damage contribution to P[SCSD] for each performance group at the recommended design points for FRC D

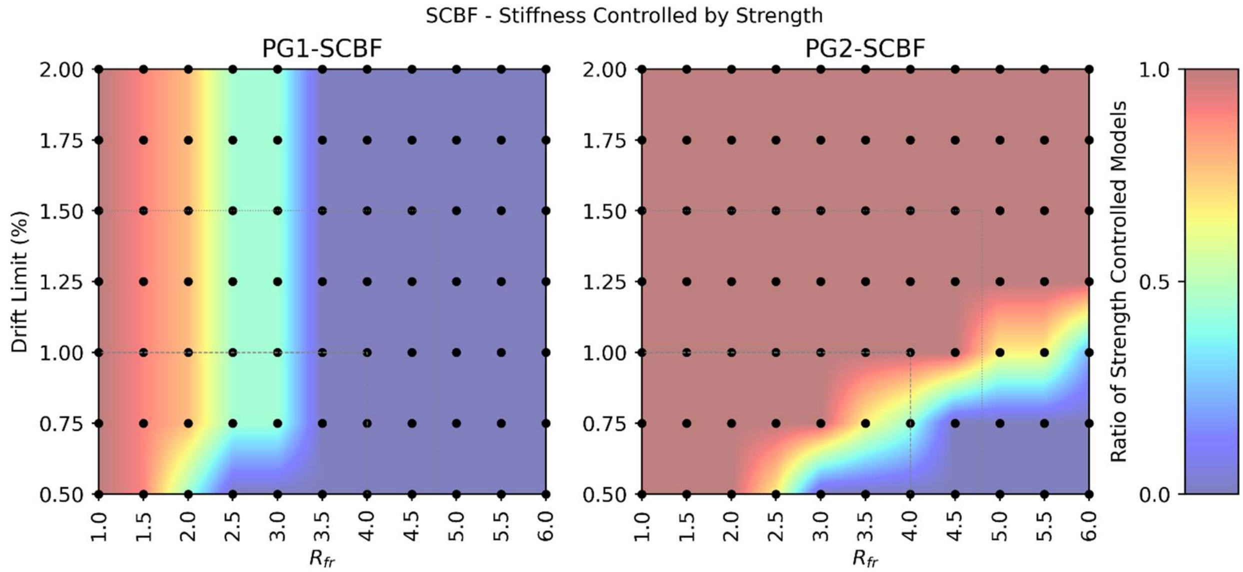

Figure 17 - Average influence of strength on building stiffness for various design requirement combinations assessed. Red coloring indicates that 100% of the models at this design point are controlled by strength requirements (e.g., tightening drift limits by one increment will not change performance). Alternately, blue coloring indicates that 100% of the models at this design point are controlled by stiffness requirements.

3.4. Validation of Peak Floor Acceleration Demand Estimates

The prequalification method documented in the 2026 NEHRP Section A.8.3.6 requires that peak floor acceleration demands be evaluated for all structural system archetype design cases to ensure that Section A.10.6 peak floor acceleration adequately reflects the actual peak floor acceleration values observed in the nonlinear response-history analysis results. If the peak floor acceleration demands exceed the acceptable limits of Section A.8.3.6, the recommended $R_{\mu fr}$ value is reduced from the baseline $R_{\mu fr}$ value to adequately adjust the peak floor acceleration demands when using the Section A.10.6 equation. The baseline $R_{\mu fr}$ values are calculated in accordance with Section 13.3.1.2 with the following modifications:

1. R_{fr} and Ω_{0fr} are used in lieu of R and Ω_0
2. The value of I_e is taken as 1.0.
3. The lower limit on $R_{\mu fr}$ of 1.3 in Equation 13.3-6 does not apply.

The recommended R_{ufr} values are determined by checking for compliance with the following two criteria:

1. The ratio of the median peak floor acceleration from analysis averaging across all structural levels to the seismic floor acceleration determined in accordance with Section A.10.7, averaged across all structural levels, is computed. The average of this ratio across all archetypes within a performance group shall not exceed 1.0.
2. The ratio of the largest peak floor acceleration from analysis at any level to the largest seismic floor acceleration determined in accordance with Section A.10.7 at any structural level is computed. The average of this ratio across all archetypes within a performance group shall not exceed 1.2.

The Section A.8.3.6 evaluation was completed, resulting in the following $R_{\mu fr}$ requirements:

- $R_{\mu fr}$ = 1.15 is required for FRC A/B/C (based on design using R_{fr} = 3.5 and Δ_{afr} = 0.75%), which is slightly smaller than the baseline value of $R_{\mu fr}$ = 1.24.
- $R_{\mu fr}$ = 1.15 is required for FRC D (based on design using R_{fr} = 4.0 and Δ_{afr} = 0.75%), which is slightly smaller than the baseline value of $R_{\mu fr}$ = 1.33.

4. CONCLUSIONS

This report documents the quantification of the functional recovery seismic performance factors for the Special Concentrically Braced Frame (SCBF) system in accordance with the proposed Section A.8.3.6 procedures of the 2026 National Earthquake Hazards Reduction Program (NEHRP) Provisions. The recommended functional recovery seismic performance factors for the SCBF are summarized in Table 12. These include the functional recovery response modification coefficient, R_{fr}, the functional recovery allowable story drift limit, $\Delta_{afr.}$, and the functional recovery structural ductility reduction factor, $R_{\mu fr}$, for estimation of peak floor accelerations. Only SCBF structures up to 10 stories tall were studied. Therefore, the recommended functional recovery performance factors are limited to SCBF structures that are 10 stories tall or less. Additionally, all SBFS systems assessed comply with new seismic compactness limits (b/t) currently under ballot for adoption into the 2027 AISC Seismic Provisions (AISC, 2025).

Results from the assessment showed that the functional recovery performance factors for SCBFs were primarily governed by a combination of local brace deformation, brace buckling, and initial weld fracture in the gusset plates, with design criteria governed by the 20% maximum acceptance criteria for the mid-rise performance group (PG2). In selecting the performance factors, preference was given to performance factor combinations with tighter drift limits and R_{fr} at or near the judgement-based limit. This approach was taken because safety-critical structural damage results from excessive displacement, and enforcing stricter drift limits is the more direct way to control displacements.

Table 12. Summary of functional recovery seismic performance factors for SCBF lateral systems up to 10 stories tall.

	FRC A/B/C			FRC D		
	R_{fr}	**Δ_{afr}***	**$R_{\mu fr}$†**	**R_{fr}**	**Δ_{afr}***	**$R_{\mu fr}$†**
Analysis results	3.5	0.75%	1.15	4.0	0.75%	1.15
Judgment-based upper limit	4	1.25%	--	5	1.75%	--
Recommendation – SCBF	**3.5**	**0.75%**	**1.15**	**4.0**	**0.75%**	**1.15**

† $R_{\mu fr}$ is only calculated for the recommended seismic performance factors.
** Drift checks are performed with C_{dfr} equal to R_{fr} for functional recovery design.*

SUPPLEMENTARY MATERIAL

Two supplementary files are attached to this Prequalification Report that provide additional detailed information on the structural response and ATC-138 outcomes from individual archetype models and performance groups, as well as performance outcomes from the independent-strength-and-stiffness check discussed in the body of the report. The general description of the content contained in each file is provided below to assist with navigation and comprehension of detailed results.

- **Analysis Report Tables** *("SupplementalData_AnalysisReportTables_SCBF_v1_3.xls")*
    - Contains detailed analysis outcomes for each archetype model assessed, including results for FRC A/B/C and FRC D.
    - "Summary" tab provides a summary of the controlling design values and other response metrics for each archetype.
    - "All Runs" tab provides response and performance outcomes for all combinations of model runs for each archetype.
- **Archetype Performance Plots** *("SupplementalData_ArchtypePerformancePlotsAppendix_SCBF_v1_3.pdf")*
    - Provides visualizations of analysis outcomes similar to the figures in the report, but for the independent-strength-and-stiffness check.
    - Provides visualizations of analysis outcomes similar to the figures in the report, but for individual archetype models.
    - Provide peak transient drift, residual drift, and peak floor acceleration response profiles for each archetype model.

REFERENCES

AISC (2022). "ANSI/AISC 341-22: Seismic Provisions for Structural Steel Buildings." American Institute of Steel Construction, Chicago, IL.

AISC (2025). Committee on Specifications Ad Hoc Task Group on Seismic Local Buckling Limits (2022-2027 cycle). *Task Group Report on: Seismic Local Buckling Limits*, American Institute of Steel Construction, Chicago, IL.

Almeter, E., Wade, K.F., Haselton, C.B., Saxey, B. (2018). "Rapid Risk Assessment of Buckling Restrained Braced Frames, With Focus on Residual Drifts," *Proceedings of the 11th U.S. National Conference on Earthquake Engineering* (11NCEE), Los Angeles, CA.

ASCE. (2022). "Minimum Design Loads and Associated Criteria for Buildings and Other Structures," *ASCE/SEI 7-22*, American Society of Civil Engineers, Reston, VA.

ASCE. (2023). "Seismic Evaluation and Retrofit of Existing Buildings." ASCE/SEI 41-23, American Society of Civil Engineers, Reston, VA.

ATC. (2021). "Seismic Performance Assessment of Buildings: Volume 8 – Methodology for Assessment of Functional Recovery Time, *ATC-138-3*, Preliminary report for FEMA P-58-8, Prepared by the Applied Technology Council for the Federal Emergency Management Agency, Washington, DC.

Blowes, K., Molina Hutt, C., Zimmerman, R., Cook, D.T., Almeter, E., Haselton, C.B. (in press). "Limiting Safety-Critical Structural Damage in Recovery-Based Seismic Design Provisions," *Earthquake Spectra*.

Burda, J., and Itani, A. (1999). "Seismic Behavior of Steel Column Base Plates." Journal of Structural Engineering, ASCE, 125(6), 653–664.

Cook, D., Wade, K., Haselton, C., Baker, J. W., & DeBock, D. J. (2018). A structural response prediction engine to support advanced seismic risk assessment. In *Eleventh US national conference on earthquake engineering, Los Angeles, CA*.

DeBock, D., Manousakis, I.V., Deierlein, G.G., Zsarnóczay, A. (2024). "Updated Model and Criteria for Residual Drift," *FEMA P-58/BD-3.7.26*, Background documentation for the ATC-138/FEMA P-58 Project, Submitted to the Applied Technology Council, Prepared for the Federal Emergency Management Agency, Washington, DC.

Deierlein, G.G., and Victorsson, I. (2008). "Fragility Functions for Steel Gravity Connections and Column Base Plates." FEMA P-58 Background Document, Prepared for the Federal Emergency Management Agency, Washington, DC.

Fahmy, M. (1999). "Seismic Performance of Exposed Steel Column Base Plate Connections." MS Thesis, University of Nevada, Reno, NV.

FEMA. (2009). “Quantification of Building Seismic Performance Factors,” *FEMA P695*, Prepared by the Applied Technology Council for the Federal Emergency Management Agency, Washington, DC.

FEMA. (2018). “Seismic Performance Assessment of Buildings: Volume 1 - Methodology,” *FEMA P-58-1*, 2nd Edition, Prepared by the Applied Technology Council for the Federal Emergency Management Agency, Washington, DC.

FEMA. (2018b). “Seismic Performance Assessment of Buildings: Volume 2 – Implementation Guide,” *FEMA P-58-2*, 2nd Edition, Prepared by the Applied Technology Council for the Federal Emergency Management Agency, Washington, DC.

Hajjar, J.F., Gomez, I., and Dexter, R.J. (2005). “Seismic Response of Steel Column Base Plate Connections.” Journal of Constructional Steel Research, 61(9), 1301–1320.

Haselton Baker Risk Group (2025). Seismic Performance Prediction Program (SP3).

Herman, D. J. (2007). “Further Improvements on and Understanding of Special Concentrically Braced Frames.” MS Thesis. University of Washington.

Liu, J., and Astaneh-Asl, A. (2000). “Cyclic Testing of Simple Connections Including Effects of Fracture.” Report No. UCB/CEE-STEEL-2000/01, Department of Civil and Environmental Engineering, University of California, Berkeley, CA.

Miranda, E. (1999). “Approximate seismic lateral deformation demands in multistory buildings,” *Journal of Structural Engineering*, **125**(4): 417-425.

Miranda, E., Reyes, C.J. (2002). “Approximate lateral drift demands in multistory buildings with nonuniform stiffness,” *Journal of Structural Engineering*, **128**(7): 840-849.

McKenna, F., Scott, M.H., Fenves, G.L. (2010). “Nonlinear Finite-Element Analysis Software Architecture using Object Composition,” *Journal of Computing in Civil Engineering*, **24**(1): 95-107.

NIST GCR 10-917-8 (2010). “Evaluation of the FEMA P-695 Methodology for Quantification of Building Seismic Performance Factors.” National Institute of Standards and Technology, Gaithersburg, MD.

Roeder, C., Lehman, D., and Lumpkin, E (2009). Fragility Curves for Concentrically Braced Steel Frames with Buckling Braces. FEMA P-58 Background Document 3.8.4. Federal Emergency Management Agency, Washington D.C.

Sen, A. D. (2014). “Seismic Performance of Chevron Concentrically Braced Frames with Weak Beams.” MS Thesis, University of Washington.

Sen, A. D. and Mrema, W. (2025). *Seismic Design Parameters for Functional Recovery of Special Concentrically Braced Frames.* Report to Sponsor: American Institute of Steel Construction.

Vamvatsikos, D., and Cornell, C.A. (2002). “Incremental Dynamic Analysis.” Earthquake Engineering and Structural Dynamics, 31(3), 491–514.

Vouvakis Manousakis, I., DeBock, D., Deierlein, G.G., and Zsarnóczay, A. (2024). “Residual Drift Demands in Modern Seismic-Resistant Structural Systems.” Earthquake Spectra, 40(2), 987–1012.